BMC Research Notes

RESEARCH NOTE

Open Access

Quantifying heterologous gene expression during ectopic MazF production in *Escherichia coli*

Nela Nikolic[1,2,3*], Martina Sauert[2], Tanino G. Albanese[2] and Isabella Moll[2*]

Abstract

Objective: MazF is a sequence-specific endoribonuclease-toxin of the MazEF toxin–antitoxin system. MazF cleaves single-stranded ribonucleic acid (RNA) regions at adenine–cytosine–adenine (ACA) sequences in the bacterium *Escherichia coli*. The MazEF system has been used in various biotechnology and synthetic biology applications. In this study, we infer how ectopic *mazF* overexpression affects production of heterologous proteins. To this end, we quantified the levels of fluorescent proteins expressed in *E. coli* from reporters translated from the ACA-containing or ACA-less messenger RNAs (mRNAs). Additionally, we addressed the impact of the 5′-untranslated region of these reporter mRNAs under the same conditions by comparing expression from mRNAs that comprise (canonical mRNA) or lack this region (leaderless mRNA).

Results: Flow cytometry analysis indicates that during *mazF* overexpression, fluorescent proteins are translated from the canonical as well as leaderless mRNAs. Our analysis further indicates that longer *mazF* overexpression generally increases the concentration of fluorescent proteins translated from ACA-less mRNAs, however it also substantially increases bacterial population heterogeneity. Finally, our results suggest that the strength and duration of *mazF* overexpression should be optimized for each experimental setup, to maximize the heterologous protein production and minimize the amount of phenotypic heterogeneity in bacterial populations, which is unfavorable in biotechnological processes.

Keywords: Bacteria, Toxin–antitoxin system, *mazEF*, Flow cytometry, Heterologous gene expression, Population heterogeneity

Introduction

MazF is the toxin part of the bacterial toxin–antitoxin MazEF module, neutralized by the MazE antitoxin and thus inactive in non-stressful conditions [1, 2]. MazF acts as an endoribonuclease that cleaves single-stranded RNA regions at ACA trinucleotide sites in *Escherichia coli* [3, 4]. As artificially produced MazF degrades the rRNA precursors, as well as mRNAs [4–8], overall translation is reduced, which leads to decline in bacterial growth [9]. Even though cells grow slowly during *mazF* overexpression, cellular processes such as transcription and translation are not halted during this growth reduction [10, 11]. A previous study has shown that bacterial populations maintain transcription during MazF production, possibly to ensure synthesis of important components of translational machinery and the antitoxin MazE, so the cells could recover from the stress rapidly [11]. Moreover, during *mazF* overexpression protein synthesis is possible from mRNAs that do not contain ACA sequences, and thus are not targeted by MazF [10]. Ectopic MazF

*Correspondence: nelanik@gmail.com; isabella.moll@univie.ac.at

[1] Institute of Science and Technology Austria (ISTA), Klosterneuburg, Austria
[2] Department of Microbiology, Immunobiology and Genetics, Max Perutz Labs, Vienna Biocenter (VBC), University of Vienna, Vienna, Austria
Full list of author information is available at the end of the article

production has been included in various experimental frameworks in biotechnology and synthetic biology. For instance, *mazF* overexpression has been employed to improve high-yield production of the protein of interest [12, 13], for manipulation of cellular resources [14], and in examining interaction networks within synthetic microbial communities [15]. In this study, we investigate how basic mRNA properties, such as the mRNA sequence and length of the untranslated region, affect synthesis of the heterologous protein during *mazF* overexpression. Additionally, this study underlines the importance of addressing the connection between expression of the gene of interest and phenotypic heterogeneity in bacterial populations during *mazF* overexpression.

Main text

Methods

Bacterial strains and reporter systems

We employed three constitutively expressed reporter systems: a plasmid-based *gfp* reporter gene devoid of ACA sites ($gfp_{\Delta ACA}$), transcribed into (1) a canonical or (2) a leaderless mRNA [16], and (3) a chromosomally encoded *mCherry* reporter gene with its native ACA sites [9]. The coding $gfp_{\Delta ACA}$ mRNA region is thus not targeted by MazF [16], while the *mCherry* mRNA is prone to the MazF-mediated cleavage [9]. Low- or high-copy plasmids harboring $gfp_{\Delta ACA}$ reporter systems were transformed into strain TB212, which is a derivative of *E. coli* BW27784 that constitutively transports L-arabinose (Ara) without metabolizing it [17]. Strain TB212 carries a chromosomally integrated *mCherry* reporter gene placed under the phage λ promoter [18], and it is additionally transformed with plasmid pBAD-*mazF* [19]. All $gfp_{\Delta ACA}$ reporter systems [16, 20], strains [17, 21] and plasmids are listed in Additional file 1: Table S1. Bacterial growth was monitored by measuring optical density at 600 nm (OD_{600}), and flow cytometry analysis was performed with LSR Fortessa (BD, USA). Detailed experimental protocols, flow cytometry setups and analyses are described in [9].

Fluorescence analysis

As a negative control for GFP and mCherry fluorescence, we measured autofluorescence of strain BW27784 pBAD-*mazF*. As an additional negative GFP fluorescence control, we employed strain TB212 pBAD-*mazF* with a $gfp_{\Delta ACA}$ reporter gene system in which a stem loop structure was placed closely upstream of the start codon to prevent ribosome binding and consequently translation, located on a high-copy or a low-copy plasmid (Additional file 2). Normalized GFP and mCherry fluorescence was calculated as the mean fluorescence level of a TB212 pBAD-*mazF* $gfp_{\Delta ACA}$ reporter strain divided by the mean fluorescence level of the reporterless strain BW27784 pBAD-*mazF*, measured at the same time point. The percentage increase in fluorescence between two measurements, e.g. between two time points t, was calculated on normalized fluorescence values as increase = [(fluorescence(t_2) − fluorescence(t_1))/fluorescence(t_1)] * 100. Error bars in all graphs present standard deviation. To evaluate differences in fluorescence datasets we used two-tailed, paired Student's *t*-test (induced vs. uninduced cultures, or 6 h-induction vs. 2 h-induction).

Sequence analysis

A 910 nucleotide-region comprising the *mazEF* locus was analyzed in the strains K-12 MG1655 (NCBI ID: U00096.3, range: 2,910,556–2,911,465), K-12 BW25113 (NCBI ID: CP009273.1, range: 2,903,915–2,904,824), and BL21(DE3) (NCBI ID: CP053602.1, range: 2,744,443–2,745,352).

Results and discussion

Low-level translation of the leaderless gfp mRNA throughout bacterial growth phases

In this study, we sought to determine how the length of the untranslated region (UTR) of an mRNA affects the synthesis of the corresponding protein throughout bacterial growth phases, and specifically during *mazF* overexpression. Bacterial canonical mRNAs harbor a 5′-UTR comprising ribosome recognition regions and other translational signals, as reviewed in [22]. Leaderless mRNAs lack 5′-UTRs or possess very short 5′-UTRs, and are, in general, translated less efficiently than canonical mRNAs. Nonetheless, previous in vitro and in vivo studies have shown that *E. coli* leaderless mRNAs can be translated by different ribosome variants [23–25]. In our experiments, we analyzed the GFP fluorescence as a proxy for translation of the leaderless $gfp_{\Delta ACA}$ reporter, referred to as ll-$gfp_{\Delta ACA}$ reporter, and the canonical mRNA $gfp_{\Delta ACA}$ reporter, referred to as can-$gfp_{\Delta ACA}$ reporter. Analysis of the ll-$gfp_{\Delta ACA}$ reporters in the early exponential phase showed that GFP fluorescence was not significantly higher in populations harboring the fluorescent reporter compared to control populations that did not carry the fluorescent reporter (Fig. 1A, B). This indicates very low ll-$gfp_{\Delta ACA}$ expression in the early exponential phase, in contrast to the higher levels of expression of the can-$gfp_{\Delta ACA}$ reporters (Fig. 1C). However, we detected an increased fluorescent signal as a result of translation of the ll-$gfp_{\Delta ACA}$ mRNA in the later phases of bacterial growth, as well as 2 and 6 h after inducing *mazF* expression (Table 1, Part A). After 2 h, GFP fluorescence of *mazF*-induced cultures increased on average by 34% compared to the respective uninduced cultures, when the ll-$gfp_{\Delta ACA}$ reporter was encoded on a high-copy

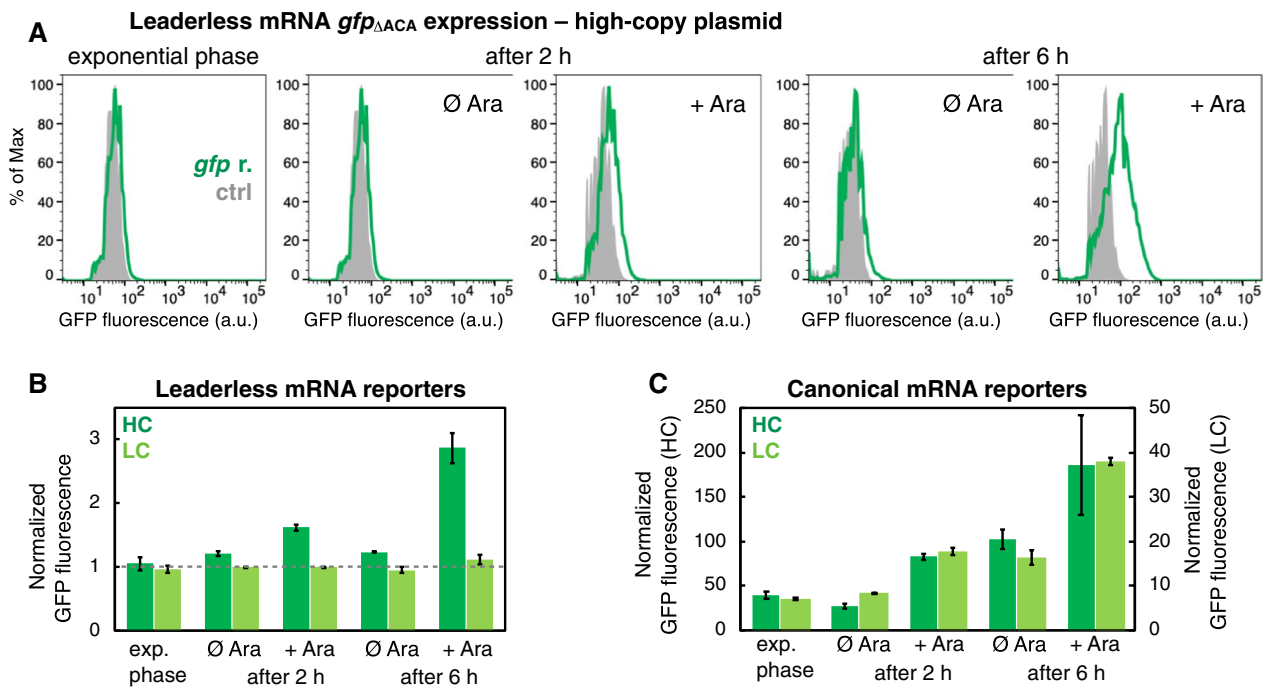

Fig. 1 Flow cytometry analysis of GFP fluorescence encoded by $gfp_{\Delta ACA}$ reporters. The leaderless mRNA of the ll-$gfp_{\Delta ACA}$ reporter entirely lacks a 5′-UTR, and this reporter construct has the start sequence ATG of the $gfp_{\Delta ACA}$ gene following directly after the promoter region [16, 20]. The canonical mRNA of the can-$gfp_{\Delta ACA}$ reporter comprises a 5′-UTR, which includes a strong ribosome binding site. **A** Green distributions depict measurements of the *E. coli* strain TB212 harboring the plasmid pBAD-*mazF* and the ll-$gfp_{\Delta ACA}$ reporter encoded on a high-copy plasmid. Light grey distributions depict measurements of the strain harboring only the plasmid pBAD-*mazF*. Here, one replicate is presented, for further results see Additional file 2. Ectopic *mazF* overexpression from plasmid pBAD-*mazF* [19] was induced by adding 0.1% Ara in the early exponential phase, at $OD_{600} = 0.18–0.22$. Flow cytometry analysis was performed in the early exponential phase, and 2 h [average OD_{600}(uninduced) = 2.45, OD_{600}(*mazF*-induced) = 0.45] and 6 h after *mazF* overexpression [average OD_{600}(uninduced) = 4.42, OD_{600}(*mazF*-induced) = 0.80]. **B** Normalized GFP fluorescence from the ll-$gfp_{\Delta ACA}$ reporters or **C** can-$gfp_{\Delta ACA}$ reporters encoded on a high-copy (HC, dark green) or a low-copy (LC, light green) plasmid, measured in different phases of bacterial growth and after adding arabinose (Ara) to induce *mazF* expression (N = 3 independent replicate cultures). Altogether, the growth of *mazF*-induced cultures was reduced by 77–86% after 2 h, and by 71–90% after 6 h, compared to the respective uninduced controls, see Additional file 2

plasmid (see "Methods" for the calculation). Six hours after *mazF* overexpression, GFP fluorescence of *mazF*-induced cultures increased by 133%. These results were further corroborated with the biochemical analysis (Additional file 3: Fig. S1). When the ll-$gfp_{\Delta ACA}$ reporter was encoded on a low-copy plasmid, GFP fluorescence of *mazF*-induced cultures did not significantly change 2 h after *mazF* overexpression, however after 6 h GFP fluorescence of *mazF*-induced cultures increased by 17%. In parallel, we analyzed GFP fluorescence encoded by the can-$gfp_{\Delta ACA}$ reporters (Fig. 1C, Table 1, Part A). Six hours after *mazF* overexpression, GFP fluorescence of *mazF*-induced cultures increased on average by 79% when the can-$gfp_{\Delta ACA}$ reporter was encoded on a high-copy plasmid (one replicate culture did not yield a significant GFP fluorescence increase), and by 134% when the can-$gfp_{\Delta ACA}$ reporter was encoded on a low-copy plasmid. In all cases, the increase in GFP fluorescence indicates the fluorescent protein synthesis and its accumulation inside bacterial cells during *mazF* overexpression. Together, this analysis suggests that translation of leaderless mRNAs occurs throughout the bacterial growth phases as well as during *mazF* overexpression, albeit at low levels.

Increased cellular concentration of GFP proteins translated from ACA-less mRNAs during mazF overexpression

We analyzed differences in fluorescence intensity of bacterial cells between two measurements during *mazF* overexpression, i.e. 2 and 6 h after inducing *mazF* expression (Fig. 2A, Table 1, Part B). We measured the fluorescence from reporter proteins encoded by the ACA-containing *mCherry*, the can-$gfp_{\Delta ACA}$ reporter genes transcribed into canonical mRNAs, as well as the ll-$gfp_{\Delta ACA}$ reporter gene transcribed into a leaderless mRNA. Our analysis shows that mCherry fluorescence increased only slightly during 4 h of *mazF* overexpression, by 35% on average (red column in Fig. 2A). In the same experimental setup, GFP fluorescence from the

Table 1 Summary table: Fluorescence increase analysis

A. Fluorescence increase of *mazF*-induced cultures compared to the uninduced cultures	**% increase**	**p-value**
Leaderless $gfp_{\Delta ACA}$ reporter		
High-copy plasmid, after 2 h	34.4 ± 2.9[a]	0.002
High-copy plasmid, after 6 h	132.8 ± 17.9	0.006
Low-copy plasmid, after 2 h	− 0.1 ± 0.6	ns[b]
Low-copy plasmid, after 6 h	17.1 ± 4.0	0.021
Canonical $gfp_{\Delta ACA}$ reporter		
High-copy plasmid, after 2 h	203.0 ± 19.0	0.0003
High-copy plasmid, after 6 h	79.4 ± 39.2	ns
Low-copy plasmid, after 2 h	112.7 ± 14.0	0.004
Low-copy plasmid, after 6 h	133.9 ± 20.2	0.001
B. Fluorescence increase during *mazF* overexpression: 6 h after induction compared to 2 h after induction	**% increase**	**p-value**
Leaderless $gfp_{\Delta ACA}$ reporter		
High-copy plasmid	77.6 ± 13.4	0.01
Low-copy plasmid	12.3 ± 6.6	ns
Canonical $gfp_{\Delta ACA}$ reporter		
High-copy plasmid	123.9 ± 60.0	ns
Low-copy plasmid	113.4 ± 5.6	1.3E−05
mCherry reporter		
Chromosomal	34.7 ± 27.9	0.001

[a] mean ± standard deviation

[b] ns stands for not significant

ll-$gfp_{\Delta ACA}$ reporter increased by 78% when the reporter was encoded on a high-copy plasmid, and by 12% when encoded on a low-copy plasmid. The highest fluorescence increase was measured for cells carrying the can-$gfp_{\Delta ACA}$ reporter: GFP fluorescence increased by 124% when the reporter was encoded on a high-copy plasmid, and by 113% when encoded on a low-copy plasmid. Firstly, the overall fluorescence increase corroborates previous findings that transcription and translation carry on during *mazF* overexpression [10, 11]. The growth rate reduction during *mazF* overexpression also indirectly contributes to the increased level of fluorescence because highly stable reporter proteins, such as GFP and mCherry, are less diluted through slower cell division [9]. Secondly, a higher fluorescence increase for cells harboring $gfp_{\Delta ACA}$ reporters indicates a higher rate of protein synthesis from mRNAs devoid of ACA sites than from ACA-containing mRNAs that can be cleaved by MazF, such as the *mCherry* mRNA, which was already implied in [10]. Finally, these results suggest considerably higher expression of proteins translated from the canonical mRNA than the leaderless mRNA form during ectopic *mazF* expression.

Interplay between gene expression and population heterogeneity during mazF overexpression

A previous study has established that fluorescence encoded by the reporter gene placed under the phage λ promoter P_R, can be employed to quantify population heterogeneity during *mazF* overexpression [9]. Specifically, differences in the reporter protein fluorescence reflect changes in the single-cell growth rate, indicating that increased variation in the growth rates of single cells within the population underlies increased population heterogeneity. In this study, population heterogeneity measured as the variation in mCherry fluorescence increased by 32% during 4 h of *mazF* overexpression (Fig. 2B). In addition, it has been previously shown that the formation of bacterial subpopulations of different fluorescent intensities occurs 5.5–6.5 h after inducing *mazF* overexpression, regardless of whether the constitutively expressed fluorescent gene reporters are encoded in the chromosome or on a plasmid [9]. Our analysis indicates that bacterial subpopulations exhibited distinct levels of can-$gfp_{\Delta ACA}$ expression 22 h after inducing *mazF* overexpression (Fig. 2C). Longer *mazF* overexpression likewise promoted larger differences in the fluorescence measurements between the replicate cultures (see error bars in Figs. 1C and 2A), and in one case even resulted

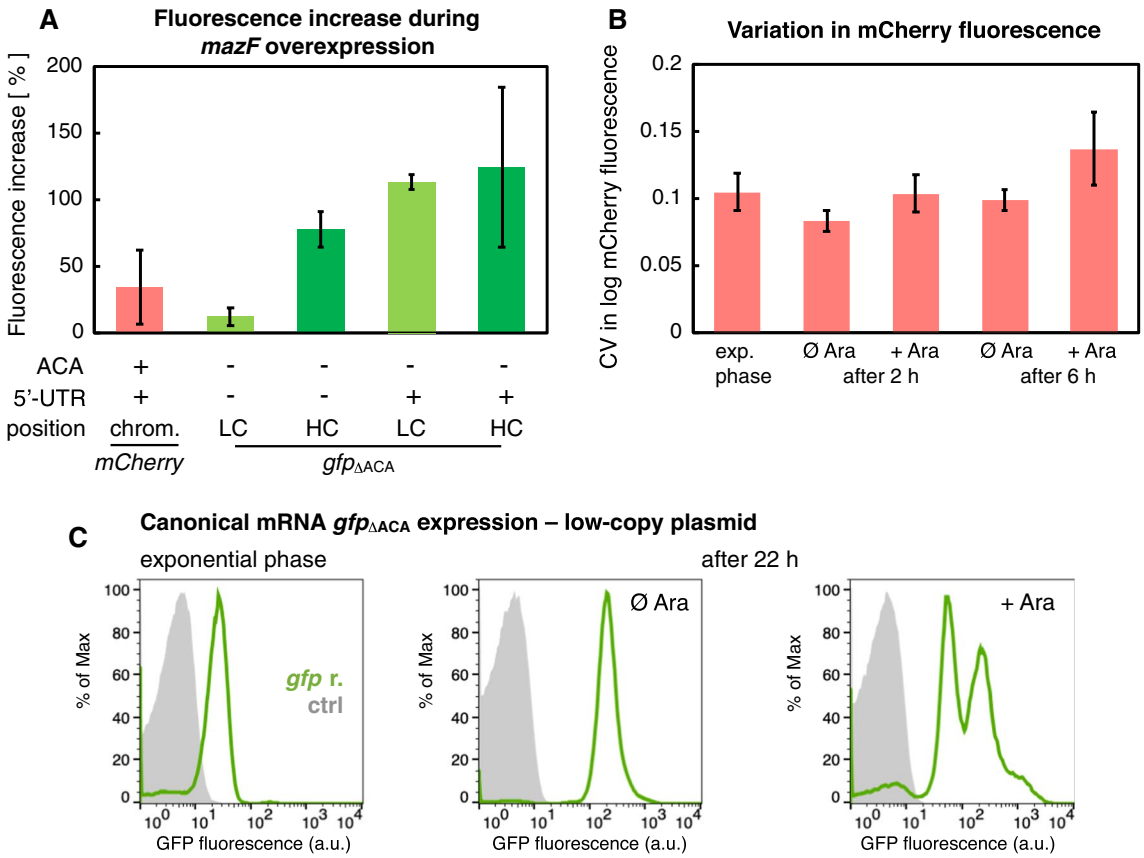

Fig. 2 Increase in the mean level and variation in fluorescence during *mazF* overexpression. **A** The increase in fluorescence of bacterial cultures was determined by comparing two flow cytometry time points, measured 2 and 6 h after inducing *mazF* expression. The fluorescent gene reporters were encoded on a high-copy (HC) or a low-copy plasmid (LC), transcribed to a leaderless (without 5′-UTR) or a canonical (containing 5′-UTR) mRNA that contained ACA sites (*mCherry*) or was devoid of ACA sites ($gfp_{\Delta ACA}$). The highest increase in fluorescence was detected from the can-$gfp_{\Delta ACA}$ reporter encoded on a high-copy plasmid, which was almost twofold higher than the fluorescence increase measured from the ll-$gfp_{\Delta ACA}$ reporter encoded on a high-copy plasmid (N = 3 independent replicate cultures for GFP fluorescence analysis, N = 12 for mCherry fluorescence analysis). **B** Coefficient of variation (CV) in mCherry fluorescence was calculated as standard deviation divided by the mean of the $\log_{10}$-transformed fluorescence data, for different phases of bacterial growth, and it is a proxy for population heterogeneity [9]. CV in mCherry fluorescence increased by 32.4 ± 19.4% in *mazF*-induced cultures, during 4 h of *mazF* overexpression (N = 12 independent replicate cultures, p-value = 0.0001). **C** Green distributions depict measurements of the *E. coli* strain BW27784 harboring the plasmid pBAD-*mazF* and the can-$gfp_{\Delta ACA}$ reporter encoded on a low-copy plasmid. Light grey distributions depict measurements of the strain harboring only the plasmid pBAD-*mazF*. 0.02% Ara was added to exponentially growing cultures to induce *mazF* overexpression, and flow cytometry analysis was performed in the early exponential phase, and 22 h after *mazF* overexpression [OD_{600}(uninduced) = 5.31, OD_{600}(*mazF*-induced) = 3.20]. After 22 h, *mazF*-induced cultures were comprised of bacterial subpopulations of different GFP fluorescence intensities, while uninduced cultures exhibited unimodal distributions of GFP fluorescence

in an insignificant fluorescence increase in can-$gfp_{\Delta ACA}$ expression (Table 1), possibly due to pleiotropic effects of *mazF* overexpression. To conclude, even though prolonged *mazF* overexpression commonly increases GFP fluorescence encoded by both ll-$gfp_{\Delta ACA}$ and can-$gfp_{\Delta ACA}$ reporters measured at the population level, it also promotes bacterial population heterogeneity.

In general, *E. coli* strains overexpressing an ACA-less gene have been used for commercial production of the respective protein under optimized fermentation conditions and *mazF* overexpression [12, 13, 26]. Recombinant protein production during *mazF* overexpression can be maintained for 3 [10], 4 [13] or even 7 days [12]. However, ectopic MazF production non-uniformly alters growth rates of bacterial cells [9]. Bacterial population heterogeneity is typically unfavorable in biotechnological processes as it reduces the yield of recombinant protein production, and causes process instability especially during large-scale cultivation [27]. Inducing *mazF* expression at lower levels or shorter periods of time has a lesser impact on the population heterogeneity [9, 28, 29]. Furthermore, one of the most widely used hosts

for recombinant protein production, *E. coli* BL21(DE3) [10, 12, 13], contains *mazEF* locus 100% identical to the *mazEF* locus of the here studied K-12 strain (see "Methods"). Therefore, a genetically engineered host *E. coli* strain with deleted *mazEF* locus could be employed in biotechnological setups, as the presence of the native *mazEF* locus has been shown to be the main source of population heterogeneity during ectopic *mazF* overexpression [9].

Conclusions

Our results show that *mazF* overexpression considerably increases cellular concentration of fluorescent proteins translated from mRNAs devoid of ACA sites. The higher reporter protein fluorescence is observed when the reporter gene is expressed at higher levels, which can be achieved by (1) employing a reporter system with a strong promoter and a strong ribosome binding site, and (2) inserting the reporter system on a high-copy plasmid. This suggests that genetic systems with different transcriptional and translational properties can be used to study cellular resource allocation during *mazF* overexpression [14]. Moreover, current efforts in synthetic biology and biotechnology focus on engineering bacterial systems with reduced phenotypic population heterogeneity [30, 31]. In order to avoid increased population heterogeneity emerging during ectopic MazF production, and to maintain the stability of recombinant protein synthesis, it is necessary to optimize experimental setups that employ MazF by adjusting the strength and duration of *mazF* overexpression.

Limitations

This study would benefit from further analysis of different types of fluorescent reporter systems in different *E. coli* strains, to provide a better understanding of the limits of experimental frameworks when employing *mazF* overexpression for the production of the specific protein and manipulation of synthetic circuits.

Abbreviations

RNA: Ribonucleic acid; mRNA: Messenger RNA; ACA sequence: Adenine–cytosine–adenine sequence; GFP: Green fluorescent protein; $gfp_{\Delta ACA}$: *gfp* Reporter gene devoid of ACA sites; ll-*gfp* reporter: Leaderless *gfp* reporter; can-*gfp* reporter: Canonical *gfp* reporter; OD_{600}: Optical density at 600 nm; Ara: Arabinose.

Supplementary Information

The online version contains supplementary material available at https://doi.org/10.1186/s13104-022-06061-9.

Additional file 1: Table S1. List of strains and plasmids.

Additional file 2. Flow cytometry data for figures.

Additional file 3: Figure S1. Analysis of the leaderless reporter. Additional methods.

Acknowledgements

We acknowledge the Max Perutz Labs FACS Facility together with Thomas Sauer. NN is grateful to Călin C. Guet for his support.

Author contributions

NN and IM designed the study; NN and MS performed the experiments; NN and TGA did data analysis; NN, TGA and IM interpreted the data; NN and IM wrote the manuscript with input from all co-authors. All authors read and approved the final manuscript.

Funding

This work was funded by the Elise Richter grant V738 of the Austrian Science Fund (FWF), and the FWF Lise Meitner grant M1697, to NN; and by the FWF grant P22249, FWF Special Research Program RNA-REG F43 (subproject F4316), and FWF doctoral program RNA Biology (W1207), to IM. Open access funding provided by the Austrian Science Fund.

Availability of data and materials

The datasets supporting the conclusions of this article are included within the article and its Additional file 2. Flow cytometry data supporting the conclusions of this article are available in the FlowRepository (http://flowrepository.org) with assigned Repository IDs: FR-FCM-Z3UV (reporter fluorescence data), FR-FCM-Z4MB (Fig. 2C) and FR-FCM-Z3VY (additional negative controls for GFP fluorescence).

Declarations

Ethics approval and consent to participate

Not applicable.

Consent for publication

Not applicable.

Competing interests

The authors declare no conflict of interest.

Author details

[1]Institute of Science and Technology Austria (ISTA), Klosterneuburg, Austria. [2]Department of Microbiology, Immunobiology and Genetics, Max Perutz Labs, Vienna Biocenter (VBC), University of Vienna, Vienna, Austria. [3]Present Address: Living Systems Institute, University of Exeter, Exeter, UK.

Received: 24 March 2022 Accepted: 28 April 2022
Published online: 13 May 2022

References

1. Gerdes K, Christensen SK, Lobner-Olesen A. Prokaryotic toxin–antitoxin stress response loci. Nat Rev Microbiol. 2005;3:371–82. https://doi.org/10.1038/nrmicro1147.
2. Yamaguchi Y, Inouye M. Regulation of growth and death in *Escherichia coli* by toxin–antitoxin systems. Nat Rev Microbiol. 2011;9:779–90. https://doi.org/10.1038/nrmicro2651.
3. Zhang Y, Zhang J, Hoeflich KP, Ikura M, Quing G, et al. MazF cleaves cellular mRNA specifically at ACA to block protein synthesis in *Escherichia coli*. Mol Cell. 2003;12:913–23. https://doi.org/10.1016/S1097-2765(03)00402-7.
4. Culviner PH, Laub MT. Global analysis of the *E. coli* toxin MazF reveals widespread cleavage of mRNA and the inhibition of rRNA maturation and ribosome biogenesis. Mol Cell. 2018;70(5):868–80. https://doi.org/10.1016/j.molcel.2018.04.026.
5. Schifano JM, Vvedenskaya IO, Knoblauch JG, Ouyang M, Nickels BE, et al. An RNA-seq method for defining endoribonuclease cleavage specificity

identifies dual rRNA substrates for toxin MazF-mt3. Nat Commun. 2014;5:3538. https://doi.org/10.1038/ncomms4538.
6. Sauert M, Wolfinger MT, Vesper O, Müller C, Byrgazov K, Moll I. The MazF-regulon: a toolbox for the post-transcriptional stress response in *Escherichia coli*. Nucleic Acids Res. 2016;44:6660–75. https://doi.org/10.1093/nar/gkw115.
7. Mets T, Lippus M, Schryer D, Liiv A, Kasari V, et al. Toxins MazF and MqsR cleave *Escherichia coli* rRNA precursors at multiple sites. RNA Biol. 2017;14(1):124–35. https://doi.org/10.1080/15476286.2016.1259784.
8. Akiyama K, Fujisawa K, Kondo H, Netsu Y, Nishikawa K, et al. MazF activation causes ACA sequence-independent and selective alterations in RNA levels in *Escherichia coli*. Arch Microbiol. 2020;202(1):105–14. https://doi.org/10.1007/s00203-019-01726-9.
9. Nikolic N, Bergmiller T, Vandervelde A, Albanese TG, Gelens L, et al. Autoregulation of *mazEF* expression underlies growth heterogeneity in bacterial populations. Nucleic Acids Res. 2018;46(6):2918–31. https://doi.org/10.1093/nar/gky079.
10. Suzuki M, Zhang J, Liu M, Woychik NA, Inouye M. Single protein production in living cells facilitated by an mRNA interferase. Mol Cell. 2005;18:253–61. https://doi.org/10.1016/j.molcel.2005.03.011.
11. Mok WW, Park JO, Rabinowitz JD, Brynildsen MP. RNA futile cycling in model persisters derived from MazF accumulation. MBio. 2015;6(6):e01588-15. https://doi.org/10.1128/mBio.01588-15.
12. Suzuki M, Roy R, Zheng H, Woychik N, Inouye M. Bacterial bioreactors for high yield production of recombinant protein. J Biol Chem. 2006;281:37559–65. https://doi.org/10.1074/jbc.M608806200.
13. Suzuki M, Mao L, Inouye M. Single protein production (SPP) system in *Escherichia coli*. Nat Protoc. 2007;2:1802–10. https://doi.org/10.1038/nprot.2007.252.
14. Venturelli OS, Tei M, Bauer S, Chan LJ, Petzold CJ, Arkin AP. Programming mRNA decay to modulate synthetic circuit resource allocation. Nat Commun. 2017;8:15128. https://doi.org/10.1038/ncomms15128.
15. Hsu RH, Clark RL, Tan JW, Ahn JC, Gupta S, et al. Microbial interaction network inference in microfluidic droplets. Cell Syst. 2019;9(3):229–42. https://doi.org/10.1016/j.cels.2019.06.008.
16. Oron-Gottesman A, Sauert M, Moll I, Engelberg-Kulka H. A stress-induced bias in the reading of the genetic code in *Escherichia coli*. MBio. 2016;7(6):e01855-16. https://doi.org/10.1128/mBio.01855-16.
17. Khlebnikov A, Datsenko KA, Skaug T, Wanner BL, Keasling JD. Homogeneous expression of the P(BAD) promoter in *Escherichia coli* by constitutive expression of the low-affinity high-capacity AraE transporter. Microbiol. 2001;147:3241–7. https://doi.org/10.1099/00221287-147-12-3241.
18. Bergmiller T, Andersson AMC, Tomasek K, Balleza E, Kiviet DJ, et al. Biased partitioning of the multidrug efflux pump AcrAB-TolC underlies long-lived phenotypic heterogeneity. Science. 2017;356(6335):311–5. https://doi.org/10.1126/science.aaf4762.
19. Amitai S, Yassin Y, Engelberg-Kulka H. MazF-mediated cell death in *Escherichia coli*: a point of no return. J Bacteriol. 2004;186:8295–300. https://doi.org/10.1128/JB.186.24.8295-8300.2004.
20. Sauert M. Selective translation of leaderless mRNAs by specialized ribosomes upon MazF-mediated stress response in *Escherichia coli*. Ph.D. Dissertation, University of Vienna, Center for Molecular Biology, Vienna, Austria. 2015. https://utheses.univie.ac.at/detail/32463/.
21. Blattner FR, Plunkett G, Bloch CA, Perna NT, Burland V, et al. The complete genome sequence of *Escherichia coli* K-12. Science. 1997;277(5331):1453–62. https://doi.org/10.1126/science.277.5331.1453.
22. Beck HJ, Moll I. Leaderless mRNAs in the spotlight: ancient but not outdated! Microbiol Spectr. 2018. https://doi.org/10.1128/microbiolspec.RWR-0016-2017.
23. Moll I, Grill S, Grundling A, Blasi U. Effects of ribosomal proteins S1, S2 and the DeaD/CsdA DEAD-box helicase on translation of leaderless and canonical mRNAs in *Escherichia coli*. Mol Microbiol. 2002;44:1387–96. https://doi.org/10.1046/j.1365-2958.2002.02971.x.
24. Moll I, Hirokawa G, Kiel MC, Kaji A, Bläsi U. Translation initiation with 70S ribosomes: an alternative pathway for leaderless mRNAs. Nucleic Acids Res. 2004;32:3354–63. https://doi.org/10.1093/nar/gkh663.
25. Byrgazov K, Vesper O, Moll I. Ribosome heterogeneity: another level of complexity in bacterial translation regulation. Curr Microbiol. 2013;16(2):133–9. https://doi.org/10.1016/j.mib.2013.01.009.
26. Yakandawala N, Gawande PV, LoVetri K, Romeo T, Kaplan JB, Madhyastha S. Enhanced expression of engineered ACA-less β-1, 6-N-acetylglucosaminidase (dispersin B) in *Escherichia coli*. J Ind Microbiol Biotechnol. 2009;36(10):1297–305. https://doi.org/10.1007/s10295-009-0613-0.
27. Heins AL, Weuster-Botz D. Population heterogeneity in microbial bioprocesses: origin, analysis, mechanisms, and future perspectives. Bioprocess Biosyst Eng. 2018;14:1–28. https://doi.org/10.1007/s00449-018-1922-3.
28. Nikolic N, Didara Z, Moll I. MazF activation promotes translational heterogeneity of the *grcA* mRNA in *Escherichia coli* populations. PeerJ. 2017;5:e3830. https://doi.org/10.7717/peerj.3830.
29. Nikolic N. Autoregulation of bacterial gene expression: lessons from the MazEF toxin–antitoxin system. Curr Genet. 2019;65(1):133–8. https://doi.org/10.1007/s00294-018-0879-8.
30. Binder D, Drepper T, Jaeger KE, Delvigne F, Wiechert W, et al. Homogenizing bacterial cell factories: analysis and engineering of phenotypic heterogeneity. Metab Eng. 2017;42:145–56. https://doi.org/10.1016/j.ymben.2017.06.009.
31. Kim J, Darlington A, Salvador M, Utrilla J, Jiménez JI. Trade-offs between gene expression, growth and phenotypic diversity in microbial populations. Curr Opin Biotechnol. 2020;62:29–37. https://doi.org/10.1016/j.copbio.2019.08.004.

Publisher's Note